CI&CEQ
Chemical Industry & Chemical Engineering Quarterly

Available on line at
Association of the Chemical Engineers of Serbia *AChE*
www.ache.org.rs/CICEQ

Chem. Ind. Chem. Eng. Q. 23 (2) 187–195 (2017) CI&CEQ

K.D. RADOSAVLJEVIĆ[1]
A.V. GOLUBOVIĆ[2]
M.M. RADIŠIĆ[3]
A.R. MLADENOVIĆ[4]
D.Ž. MIJIN[1]
S.D. PETROVIĆ[1]

[1]Faculty of Technology and Metallurgy, University of Belgrade, Belgrade, Serbia
[2]Centre for Solid State Physics and New Materials, Institute of Physics, University of Belgrade, Belgrade-Zemun, Serbia
[3]Innovation Center, Faculty of Technology and Metallurgy, University of Belgrade, Belgrade, Serbia
[4]Hemofarm A.D., STADA Company, Vršac, Serbia

SCIENTIFIC PAPER

UDC 544.526.5: 543.544:615.33:66

AMOXICILLIN PHOTODEGRADATION BY NANOCRYSTALLINE TiO_2

Article Highlights

- Nanocrystalline TiO_2 was synthesized by sol-gel route
- Nanocrystalline TiO_2 was applied in the degradation of amoxicillin
- The effect of catalyst, salt, ethanol and pH on the reaction was established
- The mineralization of amoxicillin was analyzed by IC and TOC
- The catalytic properties of nanocrystalline TiO_2 was compared to P25

Abstract

Nanocrystalline TiO_2, synthesized by sol-gel route and characterized by XRPD, BET and SEM measurements, was applied in the photocatalytic degradation of amoxicillin, using an Osram Ultra-Vitalux® lamp as the light source. Amoxicillin is a semi-synthetic penicillin type antibiotic active against a wide range of gram-positive and a limited range of gram-negative organisms. The continuous release of antibiotics and their persistence in the environment may result in serious irreversible effects on aquatic and terrestrial organisms. Heterogeneous catalysis, which uses catalysts like TiO_2, is a promising route for the degradation of organic pollutants including antibiotics. The effects of initial concentration of catalyst, initial salt concentration (NaCl and Na_2SO_4), ethanol and pH on the photocatalytic degradation of amoxicillin were studied. The mineralization of amoxicillin was analyzed by ion chromatography as well as by total organic analysis. The catalytic properties of nanocrystalline TiO_2 were compared to Evonik P25 catalyst.

Keywords: nanopowder, SEM, XRD, optimization, HPLC-MS, TOC.

From an environmental point of view, antibiotics constitute a new group of man-made chemicals of concern due to their high consumption rate worldwide. Their continuous release and persistence in the ecosystem, even at low concentrations, may result in serious irreversible effects on aquatic and terrestrial organisms. Antibiotics are an especially hazardous class of compounds, because they are potent in damaging micro-flora and fauna, they accumulate in food chains [1], and accelerate the development of resistant bacteria. Hence, antibiotics must be degraded or destroyed before discharging contingent wastewater to the environment. Central nervous system damage, mutagenic effects, nephropathy, arthropathy, light sensitivity and spermatogenesis can result from the accumulation of antibiotics in organisms [2].

Penicillin class drugs are among frequently detected antibiotics in wastewaters. However, penicillins are not usually thought to be a serious threat to the environment because of the poor stability of the β-lactam ring under pH conditions and β-lactamase activity [3]. The opening of this ring is related to the loss of microbiological activity [4,5].

Amoxicillin ($C_{16}H_{19}N_3O_5S$ (AMX), Figure 1) is a semi-synthetic penicillin type antibiotic active against a wide range of gram-positive and a limited range of gram-negative organisms. It is used in human medicine as well as in veterinary practice. The presence and fate of amoxicillin in the environment has been investigated [6,7].

Studies available in the scientific literature reported that, although usually detected in trace concen-

Correspondence: D.Ž. Mijin, Faculty of Technology and Metallurgy, University of Belgrade, Karnegijeva 4, 11120 Belgrade, Serbia.
E-mail: kavur@tmf.bg.ac.rs
Paper received: 22 January, 2016
Paper revised: 13 April, 2016
Paper accepted: 18 May, 2016

https://doi.org/10.2298/CICEQ160122030R

trations, amoxicillin continuous release into the environment increases the possibility of synergistic effects with other pharmaceuticals or chemicals in the aquatic effluent [8].

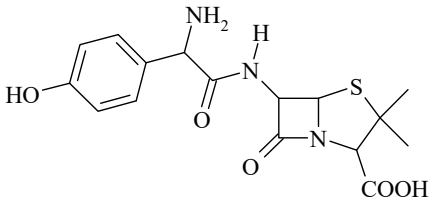

Figure 1. AMX structure.

It is useful to apply effective treatment technology to remove the amoxicillin from water. In this regard, advanced oxidation processes (AOPs), namely heterogeneous catalysis which uses catalysts like TiO_2 and ZnO, are a promising route for the degradation of organic pollutants based on the formation of hydroxyl, $^{\bullet}OH$, and other radicals and they are more suitable in comparison to other more expensive techniques, such as activated carbon adsorption, air stripping and reverse osmosis. Indeed, these techniques only transfer the pollutants from one phase to another without degrading or destroying them while AOPs radicals strongly oxidize toxic and non-biodegradable compounds to the different co-products, and, in the course of time, to innocuous end-products such as CO_2 and H_2O [9].

TiO_2 is the most commonly used photocatalyst for pollutant destruction in aqueous solution and it is very efficient – furthermore, it is inexpensive, commercially available at various crystalline forms and particle characteristics, non-toxic, stable to photocorrosion and easy to work with. The single drawback is that TiO_2 does not absorb visible light and to overcome that doping, dye sensitization, coupling and capping of TiO_2 have been studied [10].

A number of reported studies on degradation of amoxicillin by different AOPs include the treatment of amoxicillin wastewater by combination of extraction, Fenton oxidation and reverse osmosis [11]. Elmolla and Chaudhuri studied the degradation of amoxicillin, ampicillin and cloxacillin antibiotics by using Fenton [12], photo-Fenton [13] and UV/ZnO photocatalysis [14]. Degussa P-25 and other commercial as well as synthesized TiO_2 were used in the study of degradation of amoxicillin [15,16]. So, Klauson *et al.* [15] showed that aqueous photocatalytic oxidation of amoxicillin by applying TiO_2 Degussa P25 and visible light-sensitive sol-gel synthesized carbon-and iron-doped titania as photocatalysts proceeds with maximum efficiency in neutral solutions. Doped catalysts were close in efficiency to Degussa catalyst under solar radiation. Dimitrakopoulou *et al.* [16] found out that among studied photocatalysts Degussa P25 was highly active with complete AMX degradation and 93% mineralization using 10 mg dm^{-3} AMX and 250 mg dm^{-3} TiO_2 in a laboratory scale photoreactor. In general, mineralization was slower than degradation.

The aim of this work is to study the potency of sol-gel route synthesized nanocrystalline TiO_2, previously applied in the degradation of azo dye, phenol and pesticide [17], in the photocatalytic amoxicillin degradation, using an Osram Ultra-Vitalux® lamp as the light source. The catalytic property of nanocrystalline TiO_2 was compared to commercial Evonik P25 in AMX degradation. The effect of the parameters such as initial concentration of catalyst, initial salt concentration (NaCl and Na_2SO_4), ethanol and pH was analyzed. The mineralization of amoxicillin was analyzed by TOC and ion analysis.

EXPERIMENTAL

Materials

Amoxicillin trihydrate was obtained from Hemofarm-Stada. Methanol and sodium hydroxide were purchased from J.T. Baker, while acetic acid was produced by Lachner. Tetrabutyl titanate $Ti(OBu)_4$ was produced by Acros Organics, hydrochloric acid by Zorka, and ethanol by Carlo Erba. Sodium chloride was obtained from Zdravlje, and sodium sulfate from Centrochem. P25 titanium dioxide was supplied by Aldrich. All chemical used were of analytical grade or higher. All chemicals were used without further purifications. Deionized water was obtained from a Millipore water purification system.

Preparation of nanocrystalline TiO_2

The TiO_2 nanocrystals were prepared by a sol-gel method [17]. The precursor was tetrabutyl titanate and the mole ratio between reagents was $Ti(OBu)_4$:HCl:EtOH:H_2O = 1:0.3:15:4. The synthesis was carried out at the temperature of ice, where hydrochloric acid (36.2%, Zorka, Serbia), ethanol (96%, denatured, Carlo Erba, Italy), and at the end, distilled water were slowly added to tetrabutyl titanate (99%, Acros Organics, Belgium). The hydrolysis and polycondensation reactions of $Ti(OBu)_4$ were carried out at the temperature of ice. After the gelation, the wet gels were dried at 80 °C, and then the dry gels were calcined at 500 °C for 2.5 h to obtain TiO_2 nanocrystals. The heating rate and the cooling rate were the same (135 °C h^{-1}).

Photocatalytic experiment

The photodegradation of AMX was investigated in deionised water in an open reactor (100 cm³), thermostated at 25 °C [18]. For the irradiation an Osram Ultra Vitalux® 300 W lamp was used, with ratio of UV-A and UV-B lights of 13.6:3. The position of the lamp was 40 cm from the surface of the reaction mixture, containing in general AMX and TiO_2. The temperature of the reaction mixture changed for 2.5 °C during 210 min of irradiation. For every experimental cycle, 25 cm³ of the reaction mixture was placed into the reactor and stirred, using magnetic stirrer (Heidolph) for 30 min in the dark in order to reach adsorption/desorption equilibrium. Then the lamp was switched on while the continuous stirring was maintained. The aliquots were taken at defined time intervals. All the aliquots were filtrated by 0.45 μm Cronus 13 mm nylon syringe filters, in order to remove the suspended TiO_2 particles before the analysis. All the experiments were done in triplicate.

Analytical procedures

XRD

Structural analysis of prepared samples was done by XRPD on Ital Structures APD2000 diffractometer, using CuKα radiation (λ = 1.5406 Å), angular range: 20°< 2θ < 90°. Data were collected at every 0.01° in the 20-90° 2θ using a counting time of 80 s/step. MDI Jade 5.0 software was used for calculation of the structural and microstructural parameters. The Williamson-Hall method was applied for the determination of average microstrain and the mean crystallite sizes, <*D*>, of the prepared samples. The obtained values are compared to the mean crystallite sizes calculated by Scherrer formula. The Scherrer formula is an estimate crystallite size calculated from FWHM of all diffractions collected during measurement.

SEM

The morphology of the prepared TiO_2 nanopowder was analyzed by scanning electron microscope (SEM). The measurements were carried out on a Tescan MIRA3 field emission gun SEM, at 10 kV in high vacuum. SEM working distance was about 4 mm. The powder was sonicated in ethanol for 15 min. Immediately afterwards, a drop of solution was casted onto a freshly cleaved kish graphite crystal embedded with a silver paste into a sample holder. Access material was removed in a stream of argon gas and the sample was left to degas in low vacuum for 1 h, before the measurements on a scanning electron microscope. The sample plane was 40° tilted relative to the plane perpendicular to the SEM column axis.

BET

The porous structure of anatase samples is evaluated from adsorption/desorption isotherms of N_2 at -196 °C, using the gravimetric McBain method. The main parameters of the porosity, such as specific surface area and pore volume, have been estimated by BET method from α_s-plot. The pore size distribution has been estimated from hysteresis sorption data by Barret-Joyner-Halenda method.

UV and HPLC analysis

The concentration of the antibiotic was monitored by Shimadzu 1700 UV-Vis spectrophotometer at 228 nm and checked by HPLC analysis. The HPLC determinations were carried out using an HPLC instrument Agilent 1100 Series equipped with Zorbax Eclipse XDB-C18 column (Agilent). The analyses were performed in isocratic mode using water/methanol/acetic acid (200:300:5 volume ratio). The mobile phase had the flow rate of 0.8 cm³ min^{-1} and the column temperature was 258 °C. The injection volume was 5 μL and UV detection was carried out at 228 nm.

pH Measurement

The pH value of the samples was adjusted by the addition of 0.1 mol dm^{-3} NaOH or HCl and the determination of pH was performed on a Hanna HI 2210 pH meter.

Ion chromatographic analysis

Ion chromatographic analysis was performed on a Dionex DX 300 ion chromatograph at ambient temperature 25 °C with suppressed conductivity detector. The ion chromatograph was equipped with a Dionex IonPac AS14 column.

Total organic carbon analysis

Total organic carbon was measured using a Zellweger LabTOC 2100 instrument.

RESULTS AND DISCUSSION

Synthesis of TiO_2 catalyst

The TiO_2 nanocrystals can be usually obtained by a sol-gel method where titanium tetrachloride, isopropoxide titanate and tetrabutyl titanate are used as precursors [19,20]. In our study, tetrabutyl titanate ($Ti(OBu)_4$) was used as a precursor and the mole ratio between reagents were $Ti(OBu)_4$:HCl:EtOH:H_2O = 1:0.3:15:4, where hydrochloride acid was used as the catalyst, ethanol as the solvent, and water for

hydrolysis. Measured pH value of the colloidal suspension was 7. Many experiments of TiO_2 synthesis were done in order to find the optimal combination of reagents with different acids (HCl and CH_3COOH) and their various molar ratios, or different alcohols (EtOH, AmylOH), but the best combination was the mentioned one, which is in accordance to the ratio from the literature [21].

Photocatalytic properties of obtained TiO_2 were previously checked in photodegradation of textile dye C.I. Reactive Orange 16 [17] and compared to Evonik P25. The recorded activity was similar to the activity of P25 catalyst.

Characterization methods

XRPD

The most intensive diffraction peaks in the XRPD patterns of sol-gel produced sample can be ascribed to the anatase crystal structure (JCPDS card 21-1272) and it is presented, together with corresponding Miller indices, in Figure 2. There is no evidence of neither rutile nor brookite phase. Structure characteristics of our TiO_2 were: lattice parameters, a = 3.784(3) Å, c = 9.53(0) Å, V = 136.4 Å^3. Average primary particle size of 15 nm was obtained by Scherrer analyses, or 24 nm with microstrain of 0.301% obtained by Williamson-Hall method, while for Degussa P25 it was found to be 31 [22] or 20 nm [23] calculated by Scherrer equations. BET analysis revealed specific surface area (BET) of 52 m^2 g^{-1} for our sample with pore volumes 0.1063 cm^3 g^{-1} and pore diameter 5.3 nm, while data for Degussa P25 were specific surface area of 52 m^2 g^{-1} as in [22] and similar value found in the literature of 51 m^2 g^{-1} [23]. Pore volumes were 0.150 cm^3 g^{-1} and pore diameter 31.5 nm [23], where these data not cited in [22]. Therefore, it could be suggested that the specific surface area is an important parameter for the photocatalytic degradation. Degussa P25 is commercial and the most popular compound for the photocatalytic degradation. It is a combination of anatase and rutile phase (82% of anatase phase and 18% of rutile phase [22], while our sample had the pure anatase phase. One of the reasons for the synthesis of nanocrystalline TiO_2 and its comparison to Degussa P25 is the fact that one can improve the knowledge about the mechanism of photocatalytic degradation and, within the choice of offered parameters, to tailor their own process.

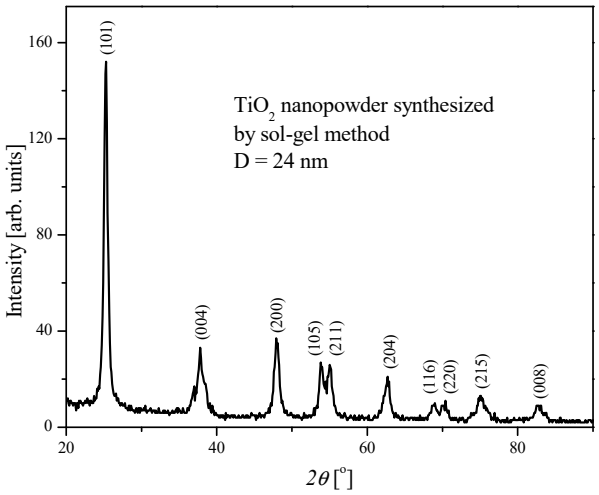

Figure 2. XRPD diffractograms of chosen TiO_2 sample together with corresponding Miller indices (JCPDS card 21-1272).

SEM

The results of SEM measurements are shown in Figure 3. Agglomerated structure could be clearly seen, which is in accordance with the fact that pH value of gel equals the point of zero charge (PZC) for TiO_2 obtained from tetrabutyl titanate [24], which promotes higher agglomeration. Values of diameters of the individual particles are in accordance with the value of the average particle size obtained by Williamson-Hall method (24 nm).

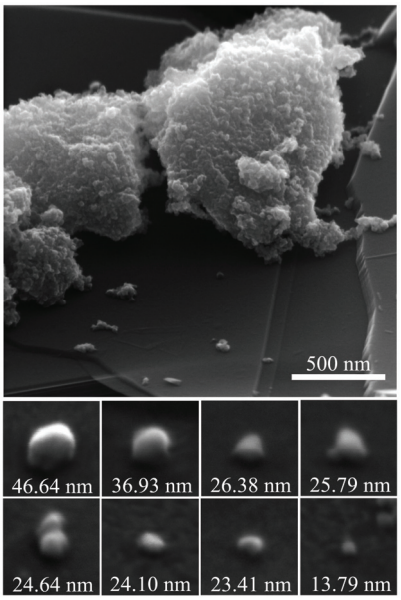

Figure 3. Top: SEM image of the conglomerated structure, also showing smaller conglomerated structures and several single particles. The top image is magnified 200×. Bottom: eight single particles. The size of each image is 100 nm×100 nm, the magnification of each bottom image is 1M×. The diameter of each particle is estimated to be within ±4 nm of the given value.

AMX photocatalytic degradation

Initial experiments

In the first experiment, the adsorption of AMX on nanocrystalline TiO_2 as well as the photolysis of AMX

was investigated (Figure 4). As can be seen, the change in normalized concentration (normalized concentration c/c_0, where c is the concentration of AMX at irradiation time t and c_0 is the initial concentration of AMX) is about 5%, indicating low adsorption (experiment in dark) of AMX on nanocrystalline TiO_2 by using the catalyst at concentration of 2 g dm^{-3}. during the photolysis of 210 min using Osram Ultra-Vitalux® 300W lamp, AMX was proven to be stable. This is in agreement with previously published literature data, where it was found that AMX is relatively stable during short reaction time in the environment as well us under simulated sunlight photolysis [6,25]. Degradation under UV light at 365 nm was ascribed to the hydrolysis rather than photolysis [26]. Due to the adsorption of AMX on nanocrystalline TiO_2, the suspension was stirred for 30 minutes in the dark prior to photocatalysis process to reach the adsorption equilibrium [27]. The equilibrium AMX concentration was then used as c_0 concentration (Figure 4). The adsorption of AMX on P25 catalyst was found to be similar to that of the prepared nanocrystalline TiO_2 (about 4%).

Consequently, the degradation of the studied antibiotic was recorded when the suspension of nanocrystalline TiO_2 and AMX was irradiated. Figure 4 shows that almost complete degradation of AMX was achieved after 210 min. The inset in Figure 4 represents the influence of the initial catalyst concentration on pseudo-first reaction constant (k). It is known that the photodegradation reaction can be well described using a pseudo-first kinetic order, which is given by the following equations [28]:

$$\ln\left(\frac{c_0}{c}\right) = kt \quad (1)$$

$$c = c_0 e^{-k\,t} \quad (2)$$

Initial photocatalyst concentration was varied in the range 0.5-4.0 g dm^{-3} and AMX concentration was 100 mg dm^{-3}. It can be seen that the photodegradation rate of AMX increased with TiO_2 concentration in the range 0.5-2.0 g dm^{-3}, presumably due to the increase in •OH production. Further increase of catalyst concentration produced a small decrease of AMX photodegradation rate. This may be due to the decreasing UV light penetration, increasing light scattering, agglomeration and sedimentation of TiO_2 at high catalyst concentration. The reaction rate may also decrease due to lessening of light density in turbid solution [29]. Based on the results, the optimum titanium dioxide concentration for degradation of AMX in aqueous suspension is 2.0 g dm^{-3}.

The catalytic property of nanocrystalline TiO_2 was compared to P25 catalyst. Figure 4 shows that in the case of AMX degradation nanocrystalline TiO_2 has similar catalytic properties as P25. This is in agreement with previously obtained results for the photocatalytic degradation of C.I. Reactive orange dye [17].

The effect of the pH value

The photodegradation of AMX was studied at five different pH values. The pH of the AMX water solution was 6. pH value of the solution was adjusted before irradiation. The adjustments of acidic (pH 3 and 5) and alkaline medium (pH 9 and 11) were made using diluted HCl or NaOH. Figure 5 reveals that

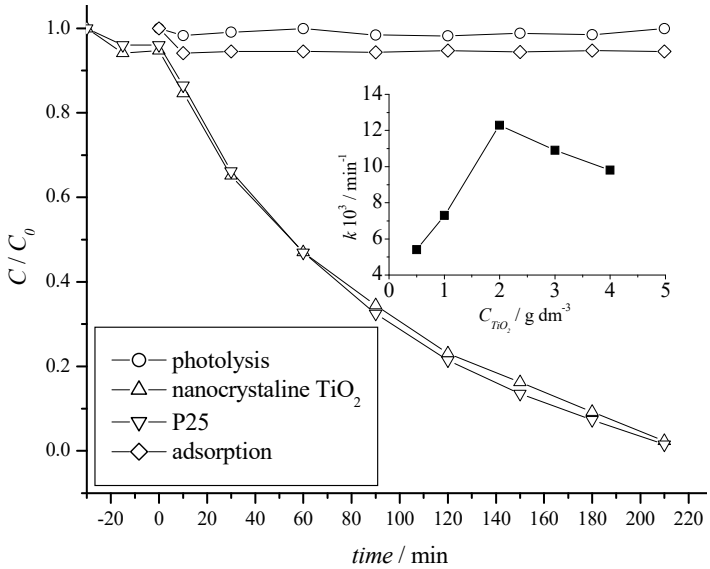

Figure 4. The effect of different experimental conditions on AMX degradation in deionised water (AMX concentration 100 mg dm^{-3}, catalyst concentration 2 g dm^{-3}). inset: influence of nanocrystalline TiO_2 concentration on the reaction rate.

increasing pH from 3 to 5/6 decreases the reaction rate. Emmola *et al*. showed that AMX is positively charged at acidic pH while at alkaline pH it is negatively charged [26]. On the other hand TiO_2 surface charge change from positive to negative. Point zero charge should be at pH 6.8 [30]. So, AMX and TiO_2 are both positively charged in acidic conditions. These should hinder the adsorption of AMX on TiO_2 surface and slow the reaction. The observed higher degradation rate (*ca*. 20%) in more acidic conditions in comparison to less acidic/neutral conditions can be explained by the hydrolysis of antibiotic as suggested earlier [31]. Increase in degradation rate (*ca*. 60%) with the increase of pH is a result of more intensive hydroxyl radical formation at higher pH on one hand, and the hydrolysis of the antibiotics, on the other. The instability of the β-lactam ring at high pH is documented in literature [32]. At alkaline pH, like in acidic, AMX and TiO_2 have the same charge (negative) so again the adsorption is hindered. The obtained results are in agreement with the previously reported effects of pH on AMX photodegradation [15,26].

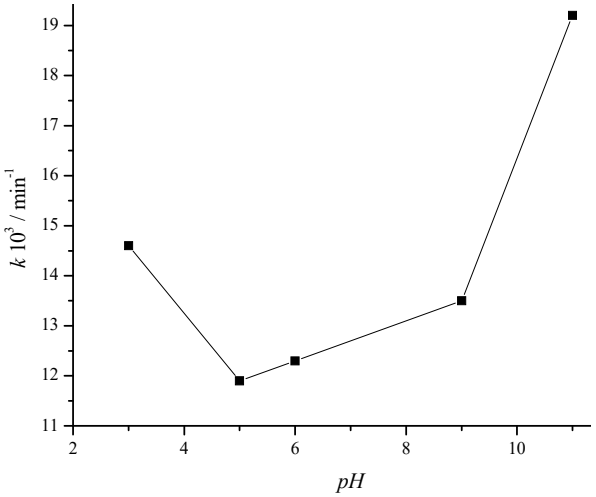

Figure 5. The effect of pH value on the photocatalytic degradation rate of AMX (100 mg dm^{-3}) in deionized water (c_{cat} = 2 g dm^{-3}).

Our photolytic experiment as well as the reported photolytic data [26] indicates the catalytic properties of the used catalyst in photodegradation of AMX. The higher observed degradation rates at low and high pH are the result of the photocatalytic effect of TiO_2 and the instability of AMX. Namely, it was found that the AMX hydrolysis rate constants, at pH 3 and 11 were 0.13 and 1.7 min^{-1}, respectively [7]. Our photocatalytic reaction rate constants, at pH 3 and 11, were found to be 14.6 and 19.2 min^{-1}, respectively. This proves the photocatalytic nature of the process.

The effect of the added salts

Inorganic ions that are usually present in wastewaters can affect the photocatalytic degradation of the organic pollutants. Inorganic anions such as carbonate, nitrate, chlorides and sulphates can have significant impact on the photodegradation reactions [18]. So, we choose to study the effect of chloride and sulphate ions on the photodegradation of AMX by using sodium chloride (NaCl) and sodium sulphate (Na_2SO_4). The influence of different concentrations of salts (20 and 200 mmol) on the photodegradation rate of AMX is presented in Figure 6.

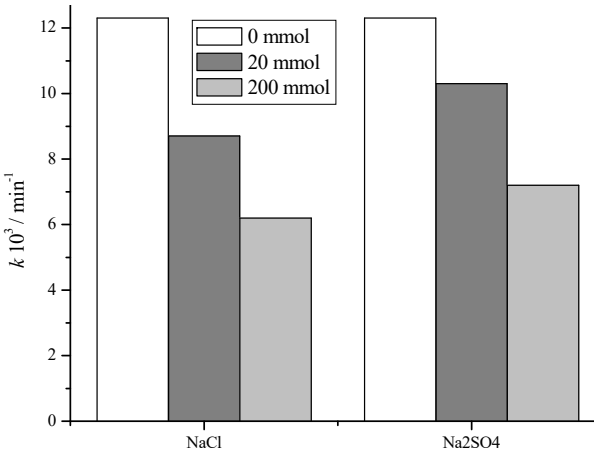

Figure 6. The effect of salts on the photocatalytic degradation rate of AMX (100 mg dm^{-3}) in the presence of nanocrystalline TiO_2 (c_{cat} = 2 g dm^{-3}).

These influences can be described by the Eqs. (3)-(9) [33-35] for chloride:

$$Cl^- + h^+ \rightarrow Cl^\bullet \quad (3)$$
$$Cl^- + {}^\bullet OH \rightarrow ClOH^{\bullet-} \quad (4)$$
$$ClOH^{\bullet-} + H^+ \rightarrow Cl^\bullet + H_2O \quad (5)$$
$$Cl^\bullet + Cl^- \rightarrow Cl_2^{\bullet-} \quad (6)$$

and sulfate:

$$SO_4^{2-} + h^+ \rightarrow SO_4^{\bullet 2-} \quad (7)$$
$$SO_4^{2-} + {}^\bullet OH \rightarrow SO_4^{\bullet-} + OH^- \quad (8)$$
$$SO_4^{\bullet-} + e_{CB}^- \rightarrow SO_4^{2-} \quad (9)$$

The observed inhibition of AMX photodegradation in Figure 6 is a result of hole scavenging properties of chloride and sulfate ions. Also there are reactions with hydroxyl radicals [36]. The observed decrease of photodegradation of AMX in the presence of chloride or sulfate anions can be explained by competitive adsorption [37]. The TiO_2 surface sites at which adsorption and electron transfer occurs can be blocked by anions thus making them effective inhibitors.

The obtained results (Figure 6) show that the chlorides are a more powerful inhibitor in comparison to sulphates, which is in accordance with previously reported results on salt effects [35]. The increase in salt concentration increases the inhibition of the reaction. While the pseudo-first reaction constant for lower sodium chloride concentration was 8.7×10^{-3} min^{-1}, the pseudo-first reaction constant for the same sodium sulphate concentration was 10.3×10^{-3} min^{-1} clearly indicating that the chloride anion is a stronger inhibitor than sulphate. The same was observed for higher concentrations (constants for sodium chloride and sodium sulphate were 6.2×10^{-3} and 7.2×10^{-3} min^{-1}, respectively).

The effect of •OH scavenger

It is known that alcohols like ethanol or methanol act as •OH scavengers [38,39], so we wanted to investigate whether the photodegradation of AMX takes place *via* •OH by adding ethanol to the reaction mixture. Ethanol was chosen because the products of the reaction are weaker oxidants (alkoxy-radicals) that react with the substrate [40].

The obtained results, given in Figure 7, clearly show that the degradation rate decreases with an increase of ethanol concentration in the reaction mixture. Addition of ethanol, in concentration of 0.69 mol dm^{-3}, decreases the reaction rate to almost half of the reaction without ethanol. This implies that •OH plays major role in photodegradation of AMX [39].

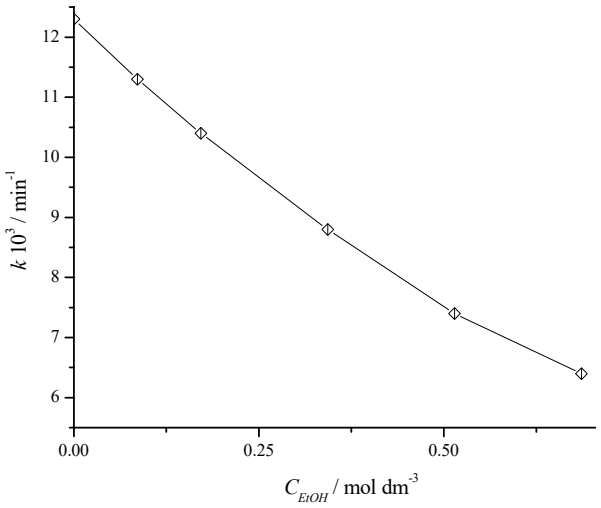

Figure 7. The effect of ethanol concentration on the photocatalytic degradation rate of AMX (100 mg dm^{-3}) in deionized water (c_{cat} = 2 g dm^{-3}).

Readings of ion chromatography and total organic carbon elimination

The mineralization of AMX was studied by ion chromatography analysis and by total organic carbon elimination. The evolutions of ionic species formed during the degradation of AMX as well as the normalized total organic carbon elimination (TOC/TOC_0) change are shown in Figure 8. The main goal of each photodegradation is the mineralization of organic molecule. Carbon and hydrogen atoms give CO_2 and H_2O, while heteroatoms give corresponding inorganic ions. Since AMX contains nitrogen and sulfur as heteroatoms, the formation of NH_4^+, NO_2^-/NO_3^- and SO_4^{2-} can be expected. Ion chromatography revealed the formation of NH_4^+, NO_3^- and SO_4^{2-} as the result of AMX degradation. According to the structure, AMX has three nitrogen atoms and one sulphur atom. For AMX, each molecule contains three nitrogen atoms, two of them in aliphatic bonds and the other in the β-lactam ring. The results showed that the initial NH_4^+ concentration was 1.1 mg dm^{-3} and after the photodegradation increased to 2.4 mg dm^{-3}. The NO_3^- concentration gradually increased from 0.26 to 1.50 mg dm^{-3}. This means that after 210 min of photocatalytic degradation about 11.2% of nitrogen was transformed – about 8.8% for NH_4^+ and 2.4% for NO_3^-. At the beginning of the reaction, concentration of sulphates was 0.42 mg dm^{-3}, while after 210 min it was 8.4 mg dm^{-3}. This indicates that about 30.4% of sulfur was mineralized. Klausen *et al.* [15] reported that AMX molecule is cleaved usually with the release of *p*-hydroxybenzoic acid or by the loss of the amino group, followed by the opening of β-lactam ring, giving at the end 3-methyl-2-oxo-3-sulfobutyric acid. Our results, which also indicate that the degradation of AMX involve the formation of carbon dioxide, water, nitrate, ammonia and sulphate anions, are in agreement with these findings.

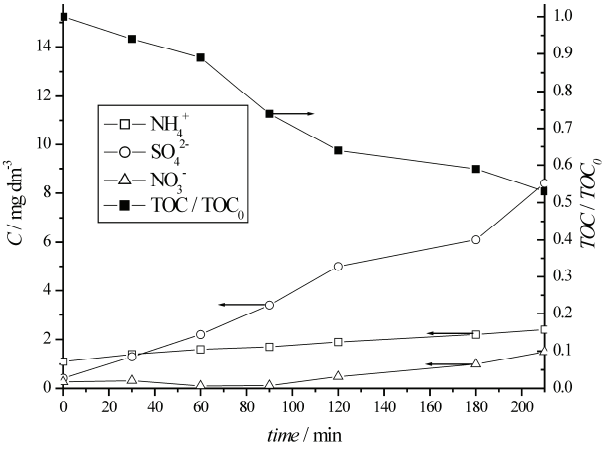

Figure 8. Time dependence of inorganic ions concentration and TOC/TOC_0 during the photocatalytic degradation of AMX (100 mg dm^{-3}) in deionized water (c_{cat} = 2 g dm^{-3}).

The mineralization of AMX was also studied by total organic carbon analysis. After 210 min of irradiation, TOC elimination was 47%, indicating that *TOC* elimination rate was not proportional to the rate of AMX disappearance and also confirms the formation of products that contain sulfur and/or nitrogen atoms.

CONCLUSION

The photodegradation of AMX was studied at five different pH values. The observed higher degradation rate in acidic conditions in comparison to neutral conditions can be explained by the hydrolysis of the antibiotic. Increase in degradation rate with the increase of pH is a result of more intensive hydroxyl radical formation at higher pH and the hydrolysis of the antibiotics. The salt effect on the photodegradation of AMX was studied by the addition of sodium chloride and sodium sulphate. The observed inhibition of AMX photodegradation is a result of hole scavenging properties of chlorides and sulfates. Addition of ethanol decreases the reaction rate, which implies that $^{\bullet}OH$ radicals play major role in photodegradation of AMX. Ion chromatography revealed the formation of NH_4^+, NO_3^- and SO_4^{2-} as the result of AMX degradation. The results showed that after 210 min of photocatalytic degradation about 11.2% of nitrogen and about 30.4% of sulfur was transformed. *TOC* elimination was 47%, indicating the formation of products that contain sulfur and/or nitrogen atoms. The catalytic property of nanocrystalline TiO_2 was compared to P25 catalyst and it was found that nanocrystalline TiO_2 has similar catalytic properties as P25.

Acknowledgement

This work has been financially supported by Ministry of Education, Science and Technological Development, Republic of Serbia, under Grant No. 172013.

REFERENCES

[1] B. Halling-Sorensen, S. Nors Nielsen, P.F. Lanzky, F. Ingerslev, H.C. Holten Lutzhoft, S.E. Jorgensen, Chemosphere **36** (1998) 357-393

[2] K. Kummerer, A. Al-Ahmad, V. Mersch-Sundermann, Chemosphere **40** (2000) 710-710

[3] M.C. Moreno-Bondi, M.D. Marazuela, S. Herranz, E. Rodriquez, Anal. Bioanal. Chem. **395** (2009) 921-946

[4] D. Li, M. Yang, J. Hu, Y. Zhang, H. Chang, F. Jin, Water Res. **42** (2008) 307-317

[5] A. Lamm, I. Gozlan, A. Rotstein, D. Avisar, J. Environ. Sci. Health, A **44** (2009) 1512-1517

[6] R. Andreozzi, V. Caprio, C. Ciniglia, M. De Champdore, R.L. Giudice, R. Marrotta, E. Zuccato, Environ. Sci. Technol. **38** (2004) 6832-6838

[7] K. Hirte, B. Seiwert, Gerrit Schüürmann, T. Reemtsma, Water Res. **88** (2016) 880-888

[8] M. Cleuvers, Ecotoxicol. Environ. Safety **59** (2004) 309–315

[9] Y. He, N.B. Sutton, H.H.H. Rijnaarts, A.A.M. Langenhoff, Appl. Cat., B **182** (2016) 132–141

[10] A.O. Ibhadon, P. Fitzpatrick, Catalysts **3** (2013) 189-218

[11] G. Zhang, S. Ji, B. Xi, Desalination **196** (2006) 32-42

[12] E. Elmolla, M. Chaudhuri, J. Hazard. Mater. **170** (2009) 666-672

[13] E.S. Elmolla, M. Chaudhuri, J. Hazard. Mater. **172** (2009) 1476-1481

[14] E.S. Elmolla, M. Chaudhuri, J. Hazard. Mater. **173** (2010) 445–449

[15] D. Klauson, J. Babkina, K. Stepanova, M. Krichevskaya, S. Preis, Catal. Today **151** (2010) 39-45

[16] D. Dimitrakopoulou, I. Rethemiotaki, Z. Frontistis, N.P. Xekoukoulotakis, D. Venieri, D. Mantzavinos, J. Environ. Manage. **98** (2012) 168-174

[17] A. Golubović, I. Veljković, M. Šćepanović, M. Grujić-Brojčin, N. Tomić, D. Mijin, B. Babić, Chem. Ind. Chem. Eng. Q. **22** (2016) 65–73

[18] D. Mijin, M. Savić, S. Perović, A. Smiljanić, O. Glavaški, M. Jovanović, S. Petrović, Desalination **249** (2009) 286–292

[19] D. He, F. Lin, Mater. Lett. **61** (2007) 3385-3387

[20] S.B. Deshpande, H.S. Potdar, Y.B. Khollam, K.R. Patil, R. Pasricha, N.E. Jacob, Mater. Chem. Phys. **97** (2006) 207-212

[21] Y.L. Du, Y. Deng, M.S. Zhang, J. Phys. Chem. Solids **67** (2006) 2405-2408

[22] A.F. Alkain, T.A. Kandiel, F.H. Hussein, R. Dillert, D.W. Bahnemann, Appl. Catal., A **466** (2013) 32-37

[23] G. Colón, M. C. Hidalgo, J. A. Navío, J. Photochem. Photobiol., A **138** (2001) 79-85

[24] M. Koslulski, Chemical Properties of Material Surface, Marcel Dekker, New York, 2001, p. 42

[25] H. Xu, W.J. Cooper, J. Jung, W. Song, Water Res. **45** (2011) 632-638

[26] E.S. Elmolla, M. Chaudhuri, Desalination **252** (2010) 46–52

[27] D.A. Lambropoulou, I.K. Konstantinou, T.A. Albanis, A.R. Fernandez-Alba, Chemosphere **83** (2011) 367-378

[28] I.K. Konstantinou, T.A. Albanis, Appl. Catal., B **42** (2003) 319–335

[29] B. Abramović, S. Kler, D. Šojić, M. Laušević, T. Radović, D. Vione, J. Hazard. Mater. **198** (2011) 123-132

[30] A. Giwa, P.O. Nkeonye, K.A. Bello, K.A. Kolawole, J. Environ. Prot. **3** (2012) 1063-1069

[31] J.P. Hou, J.W. Poole, J. Pharm. Sci. **60** (1971) 503-532

[32] A.D. Deshpande, K.G. Baheti, C.N.R. Chatterjee, Current Sci. **87** (2004) 1684-1695

[33] C. Hu, J.C. Yu, Z. Hao, P.K. Wong, Appl. Catal., B **46** (2003) 35-37

[34] N. Kashif, F. Ouyang, J. Environ. Sci. **21** (2009) 527-533

[35] O.S. Glavaški, S.D. Petrović, V.N. Rajaković-Ognjanović, T.M. Zeremski, A.M. Dugandžić, D.Ž. Mijin, Chem. Ind. Chem. Eng. Q. **22** (2016) 101–110

[36] Y. Wang, K. Lu, C. Feng, J. Rare Earths **31** (2013) 360--365

[37] D.E. Santiago, J. Arana, O. Gonzales-Diaz, M.E. Aleman--Dominiquez, A.C. Acosta-Dacal, C. Fernandez-Rodriquez, J. Perez-Pena, M. Jose, J.M. Dona-Rodriquez, Appl. Catal., B **156-157** (2014) 284-292

[38] V.N. Despotović, B.F. Abramović, D.V. Šojić, S.J. Kler, M.B. Dalmacija, L.J. Bjelica, D.Z. Orčić, Water Air Soil Pollut. **223** (2012) 3009-3020

[39] N. Daneshvar, D. Salari, A.R. Khataee, J. Photochem. Photobiol., A **162** (2004) 317-322

[40] M.R. Sohrabi, M. Davallo, M. Miri, Int. J. Chem. Tech. Res. **1** (2009) 446-451.

K.D. RADOSAVLJEVIĆ[1]
A.V. GOLUBOVIĆ[2]
M.M. RADIŠIĆ[3]
A.R. MLADENOVIĆ[4]
D.Ž. MIJIN[1]
S.D. PETROVIĆ[1]

[1]Tehnološko-metalurški fakultet Univerziteta u Beogradu, Karnegijeva 4, 11120 Beograd, Srbija
[2]Centar za fiziku čvrstog stanja i nove materijale, Institut za fiziku, Univerzitet u Beogradu, Pregrevica 118, 11080 Beograd-Zemun, Srbija
[3]Inovacioni centar Tehnološko-metalurškog fakulteta, Univerzitet u Beogradu, Karnegijeva 4, 11120 Beograd, Srbija
[4]Hemofarm A.D., Kompanija STADA, Vršac, Srbija

NAUČNI RAD

FOTODEGRADACIJA AMOKSICILINA U PRISUSTVU NANOKRISTALNOG TiO_2

Nanokristalni TiO_2 dobijen sol-gel postupkom primenjen je u fotokatalitičkoj degradaciji amoksicilina koristeći Osram Ultra-Vitalux® lampu kao izvor svetlosti. Ispitan je uticaj početne koncentracije katalizatora i soli (NaCl i Na_2SO_4), etanola i pH na reakciju. Pri proučavanju fotodegradacije amoksicilina na različitim pH vrednostima uočena je veća brzina reakcije u kiseloj sredini, u odnosu na neutralnu, što se može objasniti kiselo katalizovanom hidolizom antibiotika. Sa povećanjem pH raste i brzina reakcije kao rezultat intezivnijeg stvaranja hidroksil-radikala i bazne hidrolize antibiotika. Uticaj soli ispitivan je dodatkom natrijum-hlorida i natrijum-sulfata. Uočena inhibicija dodatkom soli posledica je dejstva hloridnih i sulfatnih jona kao hvatača šupljina. Dodatak etanola, takođe, smanjuje brzinu reakcije, što ukazuje na činjenicu da •OH imaju glavnu ulogu u fotodegradaciji amoksicilina. Jonska hromatografija je ukazala na stvaranje NH_4^+, NO_3^- i SO_4^{2-} kao rezultat degradacije amiksicilina. Dobijeni rezultati pokazuju da se oko 11,2% azota i 30,4% sumpora mineralizovalo tokom reakcije. Rezultati dobijeni određivanjem ukupnog organskog ugljenika pokazuju da je mineralizovano 47% amiksicilina i da nastali proizvodi sadrže atome sumpora i/ili azota. Poređenjem sintetisanog TiO_2 i Evonik P25 pokazano je da oba katalizatora imaju slična katalitička svojstva.

Ključne reči: nano-prah, SEM, XRD, optimizacija, HPLC-MS, TOC.